Progress In Electromagnetics Research C, Vol. 50, 131–138, 2014

Dual-Band Filter for WiMAX and WLAN with Improved Upper Stop Band Performance

Anil Kamma*, Gopi S. Reddy, Rajesh S. Parmar, and Jayanta Mukherjee

Abstract—In this paper, a novel and compact dual-band filter with enhanced upper stop characteristics has been presented. Dual band pass filter characteristics are achieved by introducing transmission zero (TZ) in pass band of band pass filter (BPF). The wide band pass filter (BPF) is implemented by combining low pass filter characteristics (i.e., stepped impedance resonator) and high pass filter characteristics (i.e., short stubs). Closed rectangular ring resonator (CRRR) and open loop rectangular ring (OLRR) combination is used to produce two transmission zeros (TZs). One TZ is placed on the pass band of BPF such that resultant filter characteristic consists of two pass band. However, the second TZ is placed at edge of the pass band in BPF to improve skirt selectivity. The two pass bands are designed to cover two popular wireless bands namely WiMAX (center frequency f_1 (3.5 GHz) and WLAN (center frequency f_2 (5.7 GHz)) bands, i.e., 3.35–3.65 GHz and 5.5–5.85 GHz respectively. Equi-ripple low pass stepped impedance resonator (SIR) filter response is responsible for improved and spurious free upper stop band (> 20 GHz, i.e., $> 6f_1$) and also provides sharp skirt attenuation at upper stop band. The proposed filter is implemented on an RT/Duroid 5880 ($\varepsilon_r = 2.2$) substrate with thickness of 0.785 mm and surface area of 19×12 sq $\cdot$ mm. Good agreement between simulated and measured results ensures that the proposed filter is a suitable candidate for modern dual band communications.

1. INTRODUCTION

Due to the demand for application flexibility and high date rate communication systems, lot of research is being done in the field of dual-band passive filters [1, 2]. In practice, dual-band filters are often employed in applications as mobile and satellite systems where application flexibility, size and weight are important constraint parameters [1–3]. Being one of the key components in communication systems, as the filters improve the performance and incorporate additional features, demand for dual band filters increases [1–3]. In addition, with the advent of the modern wireless communication technologies, single transceivers operating at multiple frequency bands have become popular [4, 5]. However, there are challenges in the design of dual-band filter supporting compact size, low insertion loss in pass bands, high quality factor and stop-band characteristics with high insertion loss and high skirt selectivity [6–10].

In [1–19], several techniques relating to planar dual-band filter design have been proposed. In particular, the commonly used approach is to use planar structures to achieve dual-band filter characteristics. The advantages of using planar dual-band filter structures are its small size, low weight and conformal nature [1–3]. Moreover, there are various methods such as meandering line and metamaterial geometry which have been reported to decrease the effective geometrical area [6, 7]. The instinctive and direct approach to realize a dual-band filter is combining two different band pass filters in parallel fashion and ensuring that both have distinct and desired pass-band characteristics [3]. Though a simple design, the effective area required using such an approach is large, and it is also cumbersome to match the impedance of both the filters [8]. Frequency transformation technique has

Received 26 April 2014, Accepted 9 May 2014, Scheduled 25 May 2014

* Corresponding author: Anil Kamma (anilkamma@ee.iitb.ac.in).

The authors are with the Department of Electrical Engineering, Indian Institute of Technology Bombay, Powai, Mumbai 400076, India.

been used to implement dual-band characteristics, but the design is complex [10]. In another simple design technique, cascade configuration of the band-pass filter and band-stop filter were used in such a manner that the resultant frequency response would be like that of a dual-band filter [1]. Stepped Impedance resonator (SIR) and coupled line resonator are commonly used configurations to realize dual-mode characteristics [10–12, 16]. In SIR configuration, dual-band filter characteristics are achieved by converting fundamental frequency mode as first resonating pass band, and its higher order modes are transformed as second pass band [12–15]. However, in this SIR configuration, designer does not have the flexibility of selecting the desired second resonant pass band. This is in contrast to coupled line resonator using multi-stub loaded resonator based dual band pass filter where designer has the choice to choose the desired first and second pass bands, but suffers from high insertion loss [2]. Another approach proposed in [9] uses defected ground structures (DGS) to achieve dual pass band filter characteristics.

All the above mentioned dual band pass filter design techniques experience undesired spurious response, which in turn affects the bandwidth of the upper stop band [10–16]. Even though [18, 19] have been designed using dual-band BPF with an improved spurious free upper stop band, they suffer from large effective geometrical area. In the present work, spurious free and wide upper stop band is achieved through compact folded SIR configuration. The proposed dual-band filter has dual-mode characteristics, which covers the two popular wireless services WiMAX and WLAN frequency bands, i.e., 3.35–3.65 GHz and 5.5–5.85 GHz respectively.

The aim of this paper is to present a planar dual-band filter and is organized as follows. Filter geometry and analysis are discussed in Section 2. Description of fabricated filter and analysis of simulated and measured results are discussed in Section 3. We have used CST microwave studio for parametric analysis.

2. DUAL-BAND FILTER STRUCTURE AND ANALYSIS

The proposed dual-band filter geometry has stepped impedance resonator (SIR), shorted stubs open loop rectangular resonator (OLRR) and closed rectangular ring resonator (CRRR) as shown in Fig. 1(a). The filter is designed on an RT/Duroid 5880 substrate with dielectric constant $\varepsilon_r = 2.2$ and thickness of substrate $h = 0.787$ mm. We also endeavor to design the proposed filter without changes in ground plane so that fabrication will be simple and compatible with other system components designed on the same substrate.

Dual-band filter characteristics should have three stop bands, i.e., upper stop band (after two pass bands), middle stop band (between pass band) and lower stop band. SIR is introduced to improve the upper stop band performance. Low-pass filter characteristics of the SIR makes the proposed filter

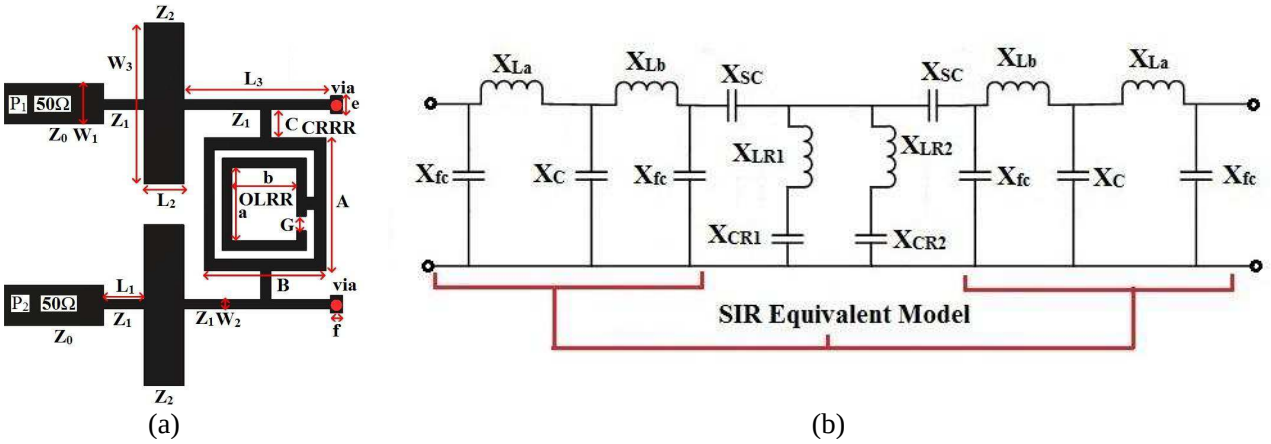

Figure 1. (a) Proposed dual band filter and its dimensions are $W_1 = 2$ mm, $W_2 = 0.5$ mm, $W_3 = 8$ mm, $L_1 = 1$ mm, $L_2 = 2$ mm, $L_3 = 7$ mm, $C = 0.9$ mm, $A = 6.8$ mm, $B = 5.6$ mm, $a = 4.4$ mm, $b = 3.8$ mm, $e = 0.8$ mm, $f = 0.4$ mm and $G = 0.7$ mm. (b) Equivalent circuit model of the proposed dual band filter.

a spurious free dual-band filter and also improves skirt attenuation rate of the upper stop band, i.e., immediately after the second pass band.

Equivalent circuit model of the proposed filter is shown in Fig. 1(b), consisting of two basic units, i.e., SIR unit and dual-band response equivalent model. SIR is modeled as series of inductor and shunt capacitor ladder network of order six. The accuracy of SIR configuration model can be further improved by incorporating associate parasitic capacitors (C_{fc1} and C_{fc3}).

With SIR being symmetrical in geometry, mathematical modeling for half of the structure is designed by using equi-ripple approach with 3-dB cutoff frequency at 6 GHz. For practical design considerations, the high impedance is taken as 106 Ω ($Z_1 = Z_{0H}$), and lowest impedance is considered as 24 Ω ($Z_2 = Z_{0L}$). Normalized element values for equi-ripple low pass response are deduced from Equation (1) [20, 21].

$$g_k = \frac{a_{k-1}a_k}{b_{k-1}b_k} \tag{1}$$

where

$$a_k = 2\sin\left\{\frac{(k-1)\,\pi}{2n}\right\} \quad k = 1, 2, \ldots, n. \tag{2}$$

$$b_k = 0.35 + \sin^2\left\{\frac{k\pi}{2n}\right\} \quad k = 1, 2, \ldots, n. \tag{3}$$

From Equations (1), (2) and (3) equivalent L and C are calculated as:

$$C_k = \frac{g_k}{Z_o\omega_c} \tag{4}$$

$$L_k = \frac{Z_o g_k}{\omega_c} \tag{5}$$

$$Z_o = \frac{60}{\sqrt{\varepsilon_{reff}}}\ln\left(\frac{8h}{w} + \frac{w}{4h}\right) \quad \text{For} \quad w/d < 1 \tag{6}$$

$$Z_o = \frac{60}{\sqrt{\varepsilon_{reff}}\,(w/h + 1.393 + 0.667\ln(w/h + 1.44))} \quad \text{For} \quad w/d \geq 1 \tag{7}$$

$$\text{And } \varepsilon_{reff} = \frac{\varepsilon_r + 1}{2} + \frac{\varepsilon_r - 1}{2}\left(1 + 10\frac{h}{w}\right)^{-1/2} \tag{8}$$

Widths of the transmission lines are computed using (6), (7), and corresponding ε_{reff} in SIR configuration are computed using (8) [20, 21]. $\varepsilon_{reff} = 1.85$, value for guided wave length (λ_d) at frequency 6 GHz is:

$$\lambda_d = \frac{\lambda_c}{\sqrt{\varepsilon_{reff}}} = \frac{3\times10^8}{6\times10^9\times\sqrt{1.85}} = 3.67\times10^{-2}\,\text{m} \tag{9}$$

$$L_a = \frac{Z_1}{\omega_c}\sin\left(\frac{2\pi L_1}{\lambda_{d\_Z0H}}\right) \tag{10}$$

$$L_b = \frac{Z_1}{\omega_c}\sin\left(\frac{2\pi L_3}{\lambda_{d\_Z0H}}\right) \tag{11}$$

$$C = \frac{1}{Z_2\omega_c}\sin\left(\frac{2\pi L_2}{\lambda_{d\_Z0L}}\right) \tag{12}$$

$$C_{fc1} = \frac{1}{\omega Z_2}\tan\left(\frac{\pi L_1}{\lambda_{d\_Z0H}}\right) \approx 67\,\text{fF} \tag{13}$$

$$C_{fc3} = \frac{1}{\omega Z_2}\tan\left(\frac{\pi L_3}{\lambda_{d\_Z0H}}\right) \approx 120\,\text{fF} \tag{14}$$

Table 1 and Table 2 show design parameters and equivalent circuit model parameters of the SIR. Low-pass filter characteristics of the designed SIR is shown in Fig. 2 (dotted lines). However, band-pass

Table 1. Parameter and dimension values for proposed structure.

	Width (w) in mm	h (mm)	w/h	ε_{reff}	λ_d (cm)
$Z_{0H} = 106\,\Omega$	0.5 mm	0.78	0.63	1.92	3.61
$Z_{0L} = 24\,\Omega$	8 mm	0.78	10.1	1.72	3.81
$Z_0 = 50\,\Omega$	2 mm	0.78	2.56	1.85	3.67

Table 2. Components of equivalent circuit.

Z_{0L}	Z_{0H}	C_{fl1}	C_{fl3}	C	L_a	L_b
24 Ω	106 Ω	67 fF	120 fF	1.438 pF	0.154 nH	0.633 nH

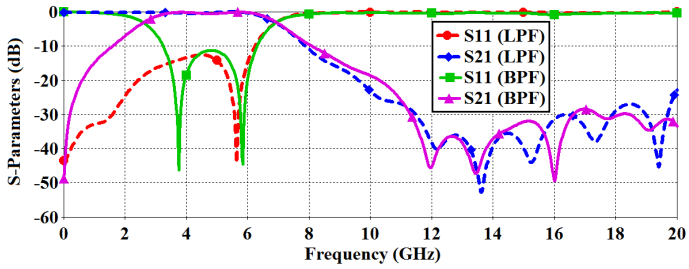

Figure 2. SIR Low pass filter characteristics (dotted lines) and band pass filter (BPF) characteristics (solid lines).

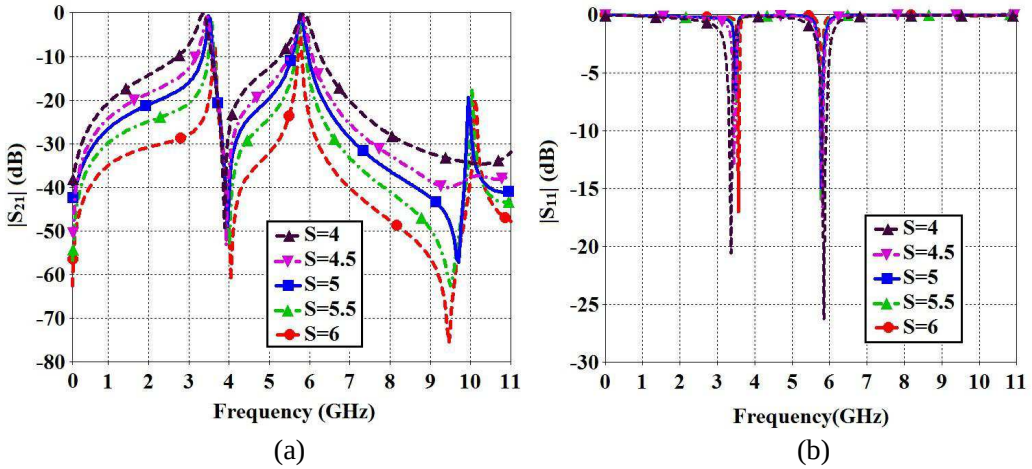

Figure 3. Parametric variations in position S of the contact C_1. (a) Transmission (S_{21}) and (b) return loss (S_{11}) characteristics of the filter.

filter response is obtained by combining designed SIR low-pass characteristics and quarter wavelength short-stub high-pass filter characteristic as shown in Fig. 2 (solid lines). As mentioned above, out of three stop bands of the dual-band filter, two stop bands are fulfilled from band-pass filter response, i.e., upper stop band and lower stop band.

In order to translate the designed BPF response into a dual pass band filter response, it is necessary to introduce middle stop band in the pass band of BPF. The middle stop band is achieved by introducing transmission zero with the help of CRRR and OLRR combination. OLRR is enclosed by the closed

rectangular ring resonator (CRRR) as shown in Fig. 1. The two open ends of the OLRR and CRRR combination behave as quarter wavelength open stubs at two different frequencies and are responsible for the two transmission zeroes in the proposed design. One transmission zero is placed at the center frequency of pass band in BPF to introduce middle stop band. However, the second transmission zero is designed at the upper stop band edge of BPF such that roll-off factor is improved.

To describe filter performance variations for parametric variation and to optimize filter parameters, parametric analyses have been carried out. The parametric analysis is associated with changing the contact position 'S'. As aforementioned, Fig. 3 shows the variation in the transmission parameter of the proposed filter for different positions, i.e., $S = 4$, 4.5, 5, 5.5 and 6 mm. The variation in the contact position leads to change in the effective electrical length of the OLRR and CRRR combination, which in turn causes shift in position of the transmission zeroes in the proposed filter characteristics. For large separation S (towards $S = 6$), it is observed that 3-dB bandwidth of two pass bands decreases, and quality factor increases. Whereas for small separation S (towards $S = 4$), it is observed that 3-dB bandwidths of two pass bands increase, and quality factor decreases. Based on above parametric analysis, the proposed filter dimensions are optimized to get desirable dual pass band characteristics. S-parameters of the optimized proposed dual-band filter is shown in Fig. 4.

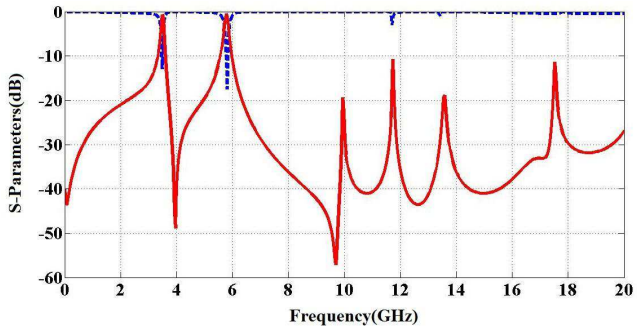

Figure 4. S-parameters of the optimized filter.

3. MEASURED RESULTS AND DESCRIPTION

The proposed dual-band filter is compact and fabricated with the surface area of 19 mm × 12 mm as shown in Fig. 5. The proposed design was implemented on an RT/Duroid 5880 substrate (dielectric constant (ε_r) 2.2 and thickness 0.785) without any modifications on the ground plane. Filter dimensions were optimized to aim at compact size and improved dual-band characteristics with wide upper stop band. The design being done only on the top layer, without any modifications on ground plane, makes the proposed filter compatible with other co-existing system components. No coupled lines in the design makes it compact and no fabrication limitation associated with closely separated coupled lines for high coupling measurements carried out on Agilent vector network analyzer, model No.-8722ET.

Simulated and measured results are shown in Fig. 6. Results depict that dual-band characteristics with improved upper stop band characteristics and the two pass bands are located at WiMAX and WLAN bands, i.e., 3.35 GHz–3.65 GHz and 5.5 GHz–5.85 GHz respectively. The measured return loss response ($|S_{11}|$) of the proposed filter at two center frequencies of the pass bands, i.e., f_1 and f_2 are 16.2 and 16.7 dB, respectively, and the corresponding insertion losses at f_1 and f_2 are 2.2 dB and 1.7 dB, respectively. The measured return losses at f_1 and f_2 are 11 dB and 6 dB higher than the corresponding simulated return loss, respectively, due to losses associated with the connectors, fabricated tolerances and dielectric losses. However, the measured return loss is better than 15 dB in the two pass bands. The upper stop band of the proposed filter is free from spurious response and also provides suppression levels of the order 20–30 dB for the complete frequency range from 6.5 GHz to 20 GHz. Table 3 shows the comparison of the present work with the recently reported merits of high in-band performance and compact size dual-band filter. It is evident from Table 3 that the proposed filter has compact and good upper stop band characteristics which is simple to design and fabricate.

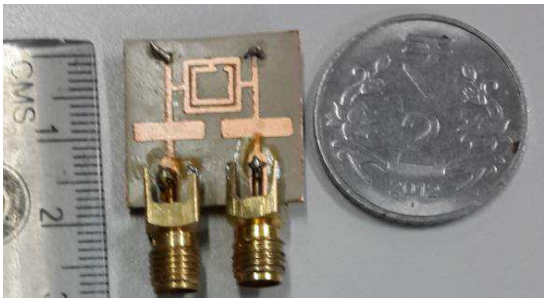

Figure 5. Fabricated proposed dual band filter.

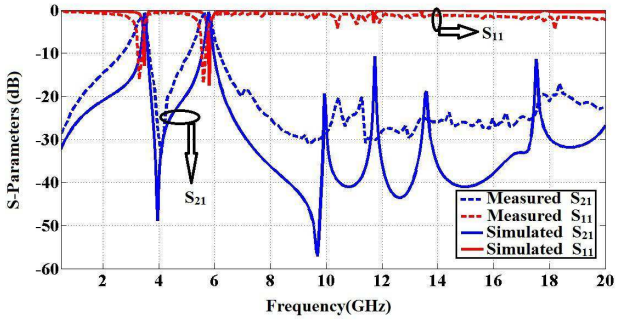

Figure 6. Measured s-parameters of the proposed filter.

Table 3. Comparison of proposed work with reported dual band filters.

	CF/IL		substrate		Effective size	F_{max}
	f_1/I_1	f_2/I_2	ε_r	h		
[1]	2.25/0.3	7.85/0.5	6.15	1.27	50×20	> 10
[2] Filter A	1.96/0.1	5.58/0.8	2.2	0.508	15.96×14.5	10
[2] Filter B	1.65/0.41	5.25/1.1	2.2	0.508	10.9×15.3	10
[4]	2.45/2.8	5.8/3.2	2.2	0.381	48×15	> 10
[8]	1.799/1.72	5.20/2	3.6	0.508	55×27	> 5
[14]	1.803/2	2.85/2.2	10.2	1.27	14.2×14.2	> 7
[15]	2.4/0.55	5.2/1.04	10.2	0.635	9.3×9.6	10
[17]	1.9/1.16	2.6/1.2	2.65	1	35×25	> 5
[18]	2.45/1.54	5.8/2.25	3.35	0.813	50×30	> 20
[19]	2.4/2.49	5.2/2.79	2.2	0.508	140×50	> 20
Present Work	3.5/1.1	5.75/0.89	2.2	0.785	19×12	> 20

$\boldsymbol{f_1/i_1}$ = first pass band center frequency/ insertion loss at f_1.
$\boldsymbol{f_2/i_2}$ = first pass band center frequency/ insertion loss at f_2.
CF/IL = center frequency of pass band and corresponding insertion loss.
$\boldsymbol{F_{max}}$ = maximum frequency for which spurious free upper stop band response is guaranteed.

4. CONCLUSION

A compact dual-band filter design has been studied and fabricated for optimized dimensional parameters. The filter has two resonant bands at WiMAX band (i.e., 3.3–3.7 GHz) and WLAN band (5.65–5.95 GHz). For dual-band characteristics, the proposed structure is composed of SIR, shorted stubs, OLRR and CRRR. SIR has been incorporated to improve the upper stop band performance of the filter by suppressing the higher order spurious components. In addition, skirt selectivity of the proposed filter is improved by low-pass characteristics of the SIR. OLRR and CRRR are responsible for two transmission zeroes, which in turn produce dual-band characteristics and form the obtained BPF. Parametric analysis is carried out to optimize the filter performance. It is found that the simulated and measured results are in fine agreement with low insertion loss and better return loss (> 15 dB). A comparative study has been done with recent reported structures supporting dual-band characteristics. The proposed compact filter is simple to design and fabricate. These merits ensure that the proposed filter is a suitable candidate for modern communication technologies.

REFERENCES

1. Marimuthu, J., A. M. Abbosh, and B. Henin, "Planar microstrip bandpass filter with wide dual bands parallel-coupled lines and stepped impedance resonators," *Progress In Electromagnetics Research C*, Vol. 35, 49–61, 2013.
2. Xu, J. and W. Wu, "Compact microstrip dual-band band-pass filter using stubs loaded coupled line," *Progress In Electromagnetics Research C*, Vol. 41, 137–150, 2013.
3. Wang, X.-H., B.-Z. Wang, and K. J. Chen, "Compact broadband dual-band bandpass filters using slotted ground structures," *Progress In Electromagnetics Research*, Vol. 82, 151–166, 2008.
4. Mondal, P. and M. K. Mandal, "Design of dual-band bandpass filters using stub-loaded open-loop resonators," *IEEE Transactions on Microwave Theory and Techniques*, Vol. 56, No. 1, 150–155, Jan. 2008.
5. Liang, F., B. Luo, W. Lu, and X. Wang, "A compact dual-band filter with close passbands using asymmetric $\lambda/4$ resonator pairs with shared via-hole ground," *Journal of Electromagnetic Waves and Applications*, Vol. 25, Nos. 8–9, 1289–1296, 2011.
6. Chen, C.-Y. and C.-C. Lin, "The design and fabrication of a highly compact microstrip dual-band bandpass filter," *Progress In Electromagnetics Research*, Vol. 112, 299–307, 2011.
7. Chen, F.-C. and J.-M. Qiu, "Dual-band bandpass filter with controllable characteristics using stub-loaded resonators," *Progress In Electromagnetics Research Letters*, Vol. 28, 45–51, 2012.
8. Chang, W.-S. and C.-Y. Chang, "Analytical design of microstrip short-circuit terminated stepped-impedance resonator dual-band filters," *IEEE Transactions on Microwave Theory and Techniques*, Vol. 59, No. 7, 1730–1739, Jul. 2011.
9. Wang, J. P., B.-Z. Wang, Y. X. Wang, and Y.-X. Guo, "Dual-band microstrip stepped-impedance bandpass filter with defected ground structure," *Journal of Electromagnetic Wave and Applications*, Vol. 22, No. 4, 463–470, 2008.
10. Guan, X., Z. Ma, P. Cai, Y. Kobayashi, T. Anada, and G. Hagiwara, "Synthesis of dual-band bandpass filters using successive frequency transformations and circuit conversions," *IEEE Microwave and Wireless Components Letters*, Vol. 16, No. 3, 110–112, Mar. 2006.
11. Ha, J., S. Lee, B.-W. Min, and Y. Lee, "Application of stepped-impedance technique for bandwidth control of dual-band filters," *IEEE Transactions on Microwave Theory and Techniques*, Vol. 60, No. 7, 2106–2114, Jul. 2012.
12. Ruiz-Cruz, J. A., M. M. Fahmi, and R. R. Mansour, "Triple-conductor combline resonators for dual-band filters with enhanced guard-band selectivity," *IEEE Transactions on Microwave Theory and Techniques*, Vol. 60, No. 12, 3969–3979, Dec. 2012.
13. Sun, S. and L. Zhu, "Compact dual-band microstrip bandpass filter without external feeds," *IEEE Microwave and Wireless Components Letters*, Vol. 15, No. 10, 1531–1309, Oct. 2005.
14. Gorur, A. K. and C. Karpuz, "A novel perturbation arrangement for dual-mode resonators and its dual-band bandpass filter applications," *Proceedings of the 41st European Microwave Conference*, 468–471, 2011.
15. Kuo, J.-T. and S.-W. Lai, "New dual-band bandpass fiter with wide upper rejection band," *Progress In Electromagnetics Research*, Vol. 123, 371–384, 2012.
16. Wang, J., H. S. Ning, Q. X. Xiong, M. Q. Li, and L. F. Mao, "A novel miniaturized dual-band bandstop filter using dual-plane defected structure," *Progress In Electromagnetics Research*, Vol. 134, 397–417, 2013.
17. Deng, K., S. Yang, S. J. Sun, B. Wu, and X. W. Shi, "Dual-mode dual-band bandpass filter based on square loop resonator," *Progress In Electromagnetics Research C*, Vol. 37. 119–130, 2013.
18. Mashhadi, M. and N. Komjani, "Design of dual-band band-pass filter with wide upper stopband using SIR and GSIR structures," *Progress In Electromagnetics Research C*, Vol. 32, 221–232, 2012.
19. Kuo, J.-T. and H.-P. Lin, "Dual-band band-pass filter with improved performance in extended upper rejection band," *IEEE Transactions on Microwave Theory and Techniques*, Vol. 57, No. 4, 824–829, Apr. 2009.

20. Fooks, E. H. and R. A. Zakareviius, *Microwave Engineering Using Microstrip Circuits*, Prentice Hall, 1990.
21. Pozar, D. M., *Microwave Engineering*, 2nd edition, John Wiley & Sons, Inc., 1998.